

Research Article

# Applications of Innovative Polygon Trend Analysis and Trend Polygon Star Concept Methods for the Variability of Precipitation at Synoptic Stations in Benin (West Africa)

Hilaire Kougbegbede\* , Mamadou Wa ïli Onah , Arnaud Houeto ,  
Ferdinand Sourou Hounvou 

Laboratory of Material Sciences and Modelisation, University of Abomey-Calavi, Abomey-Calavi, Benin

## Abstract

Climate variability poses new risks and uncertainties. In the sub-Saharan region, the impacts are already being felt and represent an additional level of obstacles for most vulnerable people, as well as a threat to sustainable development. This study analyzes the variability of precipitation in Benin using new approaches. The precipitation data used is the monthly average recorded at synoptic stations from 1970 to 2019 by the Met éo-B énin agency. Two innovative graphical trend methods, innovative polygon trend analysis (IPTA) and trend polygon star concept (TPSC), are applied to the data. Both methods allow for the assessment of periodic characteristics of the monthly average rainfall and visually interpreting the transition trends between two consecutive months. The results show that the average monthly precipitation does not follow a regular pattern. There is also a general upward trend in precipitation for most months at the stations used. Most TPSC arrows were found in regions I and III. According to the TPSC graphs, the longest transition arrows between two consecutive months were observed in quadrant III. They were noted between the months of June and July in Cotonou, October and November in Bohicon and Save, and between September and October for the remaining stations. The results of this study are of great importance for policies regarding ongoing climate change in the agricultural, health, economic, security, and environmental sectors.

## Keywords

IPTA, TPSC, Polygonal Trends, Climate Change, Rainfall Trends, Benin, West Africa

## 1. Introduction

One of the major challenges of the 21st century for the entire world is to keep global warming below 2 °C ([1]). The impacts of global warming are manifesting worldwide through violent tornadoes, extreme rainfall, heatwaves, and increasingly prolonged dry spells [2]. In Africa, the effects of climate change are becoming more acute, resulting in floods, heatwaves, and droughts with increased frequency and inten-

sity [3]. These weather phenomena lead to water shortages, fuel desertification, accelerate coastal erosion, damage infrastructure, reduce crop yields, and contribute to revenue losses for states [3-5].

Moreover, rapid urbanization and population growth in many African cities intensify pressure on infrastructure and basic services, making populations even more vulnerable to

\*Corresponding author: [hilaire.kougbegbede@uac.bj](mailto:hilaire.kougbegbede@uac.bj) (Hilaire Kougbegbede)

Received: 22 October 2024; Accepted: 9 November 2024; Published: 28 November 2024



Copyright: © The Author(s), 2024. Published by Science Publishing Group. This is an **Open Access** article, distributed under the terms of the Creative Commons Attribution 4.0 License (<http://creativecommons.org/licenses/by/4.0/>), which permits unrestricted use, distribution and reproduction in any medium, provided the original work is properly cited.

extreme weather events [6]. Agricultural impacts are evident; for instance, Niang et al. (2014) demonstrated that in the Sahel [7], the effects of global warming are already visible through soil degradation and reduced water resources, making life precarious for millions. The yields of staple crops are also affected by warming. Indeed, staple crop yields could decrease by 5 to 10% [6]. Thus, smallholder farmers, who rely on stable climate conditions for their production, find themselves particularly vulnerable to these changes and are forced to migrate [8]. Research agrees that climate change can be a significant factor driving migration [9, 10]. According to these studies, migration will intensify and may lead to insecurity, human rights violations [9], numerous social and economic tensions within the region [11, 12], and school dropouts, among other issues.

In Benin, a country in West Africa, several studies have focused on analyzing climate warming and its impacts, often followed by proposals for adaptation methods. Although the attribution to climate change is not yet formal, there is a consensus that temperature and rainfall are subject to significant variability, which ultimately impacts several sectors [13], notably the ecosystem [14]; water resources [15]; electricity production [13, 16]; and agriculture [17, 18].

Starting from the table painted above, monitoring meteorological parameters through the determination and analysis of their trends is more than essential, especially to demonstrate climate evolution in a given location [19]. Rainfall is one of the key parameters most commonly used to assess climate variability [20]. It is often used due to its importance in human life and the environment [21, 22]. Examples include hydroelectric production, agriculture, groundwater recharge, and its influence on the hydrological cycle [13, 23]. Therefore, planning activities in the various areas that rely on rainfall in a given region necessitates a thorough analysis of rainfall variability in that location. One common method is trend analysis [24]. This is done through several traditional methods, notably the Mann-Kendall method [25, 26] and linear regression [27]. Although they are the most commonly used, traditional methods have several limitations that can affect the accuracy and relevance of the results [28-32]. Recently, innovative methods based on graphical tools have been proposed to improve the accuracy and reliability of hydrometeorological variable trends [33-36]. Unlike traditional methods, graphical methods do not require any assumptions [34, 35]. The most recent of the graphical methods is the polygon method (IPTA) proposed by [37] and later improved [38]. This method, named IPTA and TPSC, not only identifies hidden trends but also facilitates the comparison of trends both in similar sites and across different climatic zones [20, 37-40]. It also highlights the interconnection of rainfall from one month to another [38]. The works of Qadem and Tayfur [41-44] demonstrate the utility of the IPTA method not only for precipitation but also for other climatic variables, showing that integrating these methods can enrich our understanding of complex climatic dynamics. The objective of this study is to investigate

the trends of monthly rainfall in Benin. We will subsequently present (i) the data and methods and (ii) the results and discussion.

## 2. Data and Methods

### 2.1. Data

In this study, the rainfall data used are collected from synoptic stations across Benin over a significant period of time by the Météo-Bénin agency, which is responsible for meteorology data collection in the country. The data for this study cover the years 1970-2019, amounting to fifty years of collection. It was noted that there is one year of missing data in Natitingou. The synoptic stations have fewer missing data and play a crucial role in the collection of meteorological data in various regions of the country. In Benin, a country characterized by diverse climatic zones, these stations provide rich datasets that can shed light on local climate patterns and trends, as evidenced by their distribution across the territory (Figure 1).

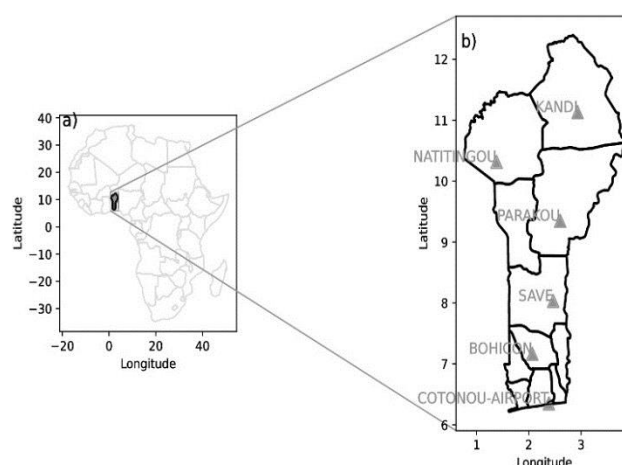


**Figure 1.** (a) Position of Benin on the map of Africa and (b) location of synoptic stations on the map of Benin.

### 2.2. Methods

In this study, the innovative polygonal trend analysis (IPTA) method and the trend polygon star concept (TPSC) method are applied to monthly average rainfall to highlight the rainfall trend at each station.

#### 2.2.1. IPTA Method

The IPTA method consists of five points [20]. However, before detailing each step, the data from each station is organized in a matrix format (Equation 1), where the rows represent the number of years of data collected and the columns represent the periods for which trends are to be evaluated

(monthly, dekadal, or seasonal). In our study, the accumulation periods are the different months of the year.

$$R = \begin{bmatrix} x_{1,1} & \cdots & x_{1,12} \\ \vdots & \ddots & \vdots \\ x_{n,1} & \cdots & x_{n,12} \end{bmatrix} \quad (1)$$

The resulting matrix is divided into two parts. The first part spans from year 1 to year  $n/2$ , while the second part covers from year  $n/2 + 1$  to year  $n$ . The means and standard deviations of the first sub-matrix are constructed with those of the second sub-matrix in a Cartesian coordinate system. The data from the first sub-matrix are plotted on the x-axis, and those from the second on the y-axis (see Figure 2). The different points are connected to form a polygon as indicated in Figure 2. Months below the 1:1 line show that the monthly totals of the second period are decreasing compared to those of the first period. Similarly, months above the 1:1 line indicate an upward trend in the totals of the second period compared to the monthly totals of the first. Those aligned along the 1:1 line show no noticeable trend. The distribution of rain affects the shape of the resulting polygon. More complex shapes can be expected to describe the precipitation behavior in the region (Sen, 2019).

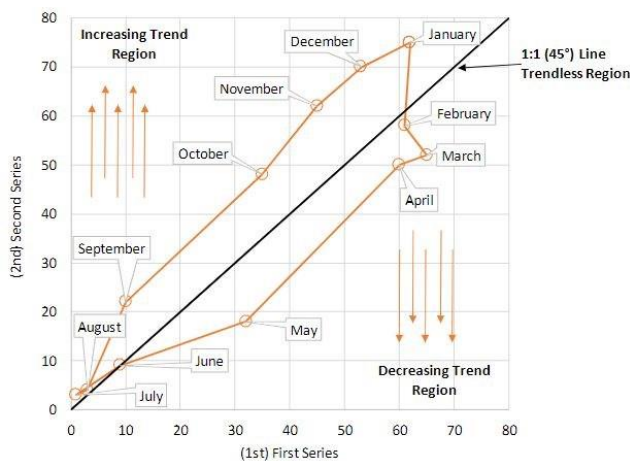


Figure 2. An innovative polygon trend analysis (IPTA) template for monthly records [20].

- The various steps for analyzing the data are as follows [20]:
- 1) the monthly rainfall time series is divided into two equal parts;
  - 2) for each month in both sub-periods, the mean is calculated;
  - 3) on the horizontal (vertical) axis of the scatter plot, the first (second) period is located on the x-axis (y-axis), and 12 points are plotted to represent the 12 months;
  - 4) a polygon is created by connecting the points;
  - 5) The distance and slope of the line connecting two consecutive points are calculated using the formulas below:

$$d_{AB} = \sqrt{(x_B - x_A)^2 + (y_B - y_A)^2} \quad (2)$$

$$S_{AB} = \frac{y_B - y_A}{x_B - x_A} \quad (3)$$

$x_A$  and  $x_B$  ( $y_A$  and  $y_B$ ) are derived from the first (second) sub-period and represent the x-coordinates (y-coordinates) of the two consecutive points A and B.  $d_{AB}$  indicates the rainfall shift between two successive months, while  $S_{AB}$  shows the increase of the second sub-period compared to the first. The steeper the slope, the greater the monthly variation in the second sub-period compared to the first, and vice versa.

When the variability is homogeneous between successive points, the polygon will exhibit a regular shape, meaning that the lengths and slopes will be the same for successive points. Under these conditions, the variability of the hydrometeorological variable is isotropic and uniform [37, 40]. Conversely, the more complex the shape of the polygon, the more complex the variability of the hydrometeorological variable will be between successive months at the station considered.

### 2.2.2. TPSC Method

The TPSC is a star graph that highlights the transition between consecutive points describing the polygon obtained with IPTA [38]. Through this representation, the distance between two successive points and the slope of the line connecting these two points are directly appreciable to the naked eye.

The vectors representing the transition between two successive points are drawn from the origin (0:0) of the Cartesian coordinate system. For a vector depicting the transition between two successive points, the x-coordinate (y-coordinate) corresponds to the difference between the values of these two points in the first (second) sub-period. The length of the vector indicates the extent of the transition between the two points. The smaller (larger) the vector length, the smaller (larger) the transition between two successive points will be. The horizontal (vertical) projection of each vector represents the magnitude of the change in the first (second) sub-period. The change in monthly rainfall is determined by comparing the vertical and horizontal projections of the vector. The slope of the change is obtained by the ratio of the vertical to horizontal projections of the transition vector.

Figure 3 shows an example of TPSC. The vectors in region I (III) indicate an upward (downward) trend in monthly rainfall in both sub-periods. Quadrant II (IV) represents an upward (downward) trend in the second (first) sub-period compared to the first (second) sub-period.

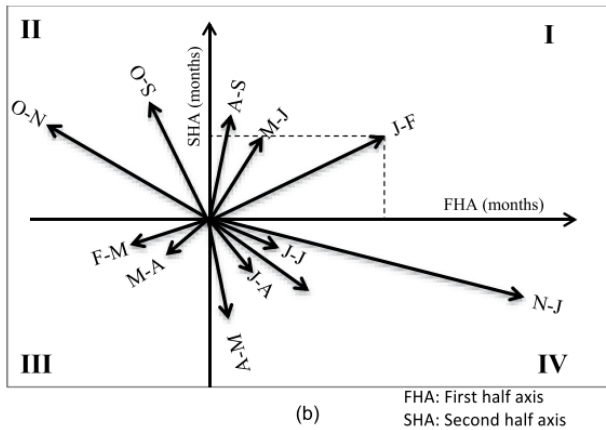


Figure 3. TPSC example [38].

### 3. Results and Discussion

#### 3.1. Results

The IPTA and TPSC tests are applied to the monthly av-

erage rainfall data from six synoptic stations. The rainfall distances and slopes between successive months at each of the six stations are presented in Table 1. Overall, the IPTA graph indicates that the monthly average rainfall does not follow a regular pattern. The highest average monthly totals are recorded in the second sub-period, except in Parakou, where no change was observed. The highest monthly totals were recorded in July at Bohicon (164.04 mm), in June at Cotonou (345.07 mm), and in September at Save (175.39 mm). As for the three other stations located further north in the country, the highest total was recorded in August: 272.96 mm in Kandi, 281.07 mm in Natitingou, and 218.74 mm in Parakou. The TPSC graphs, on the other hand, show that the rainfall transitions from one month to the next behave almost similarly from station to station. The majority of vectors occupy regions I and III. The slope value indicates the sub-period where the trend is relatively higher. Regardless of the area, when the absolute value of the slope is greater (less) than 1, the trend is more significant in the second (first) sub-period. Next, we present the analysis by station.

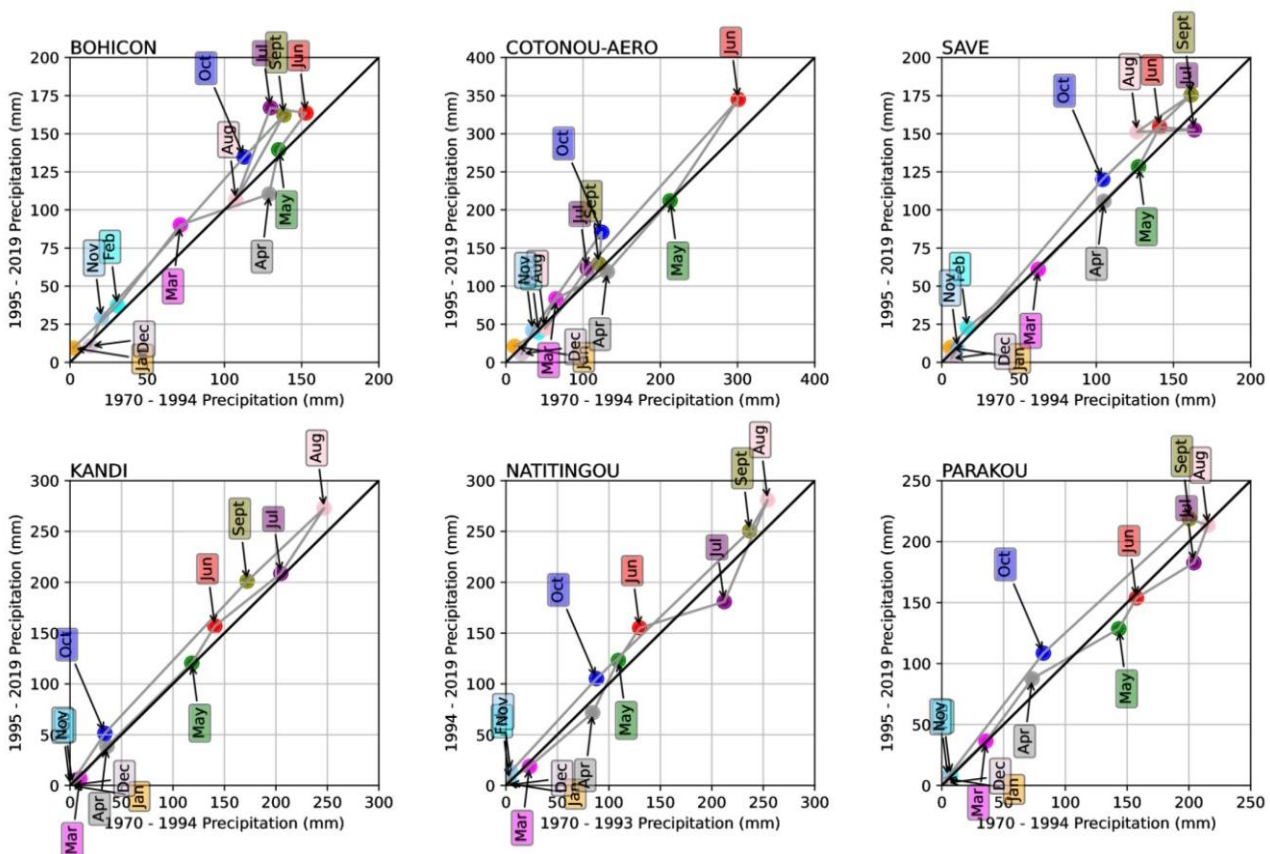


Figure 4. IPTA test at each station.

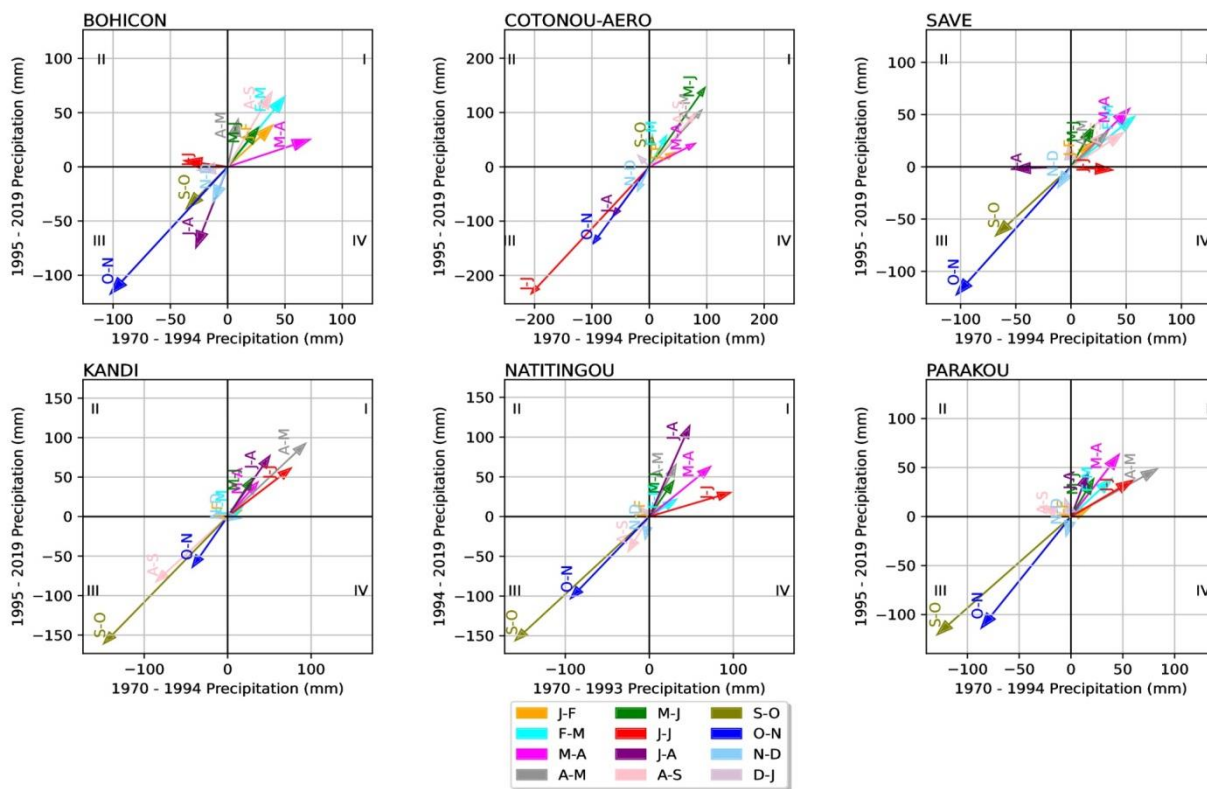


Figure 5. TPSC test at each station.

Table 1. Rainfall distance and trend slope between successive months at each station.

		Jan-Feb	Feb-Mar	Mar-Apr	Apr-May	May-June	Jun-Jul	Jul-Aug	Aug-Sept	Sept-Oct	Oct-Nov	Nov-Dec	Dec-Jan
BOHICON	TL	39.83	66.83	61.04	29.73	29.92	23.21	64.47	63.74	37.63	140.46	19.68	11.09
	Slope	0.98	1.30	0.35	4.80	1.36	-0.15	2.69	1.79	1.07	1.14	2.54	0.12
COTONOU-AERO	TL	36.25	49.20	75.44	123.53	159.72	295.94	95.87	110.07	41.52	156.99	33.83	13.47
	Slope	0.60	1.94	0.54	1.14	1.51	1.13	1.44	1.22	11.01	1.44	2.15	-1.07
SAVE	TL	16.98	59.73	61.68	31.92	29.32	22.55	37.07	42.51	79.71	145.19	7.93	7.22
	Slope	1.19	0.84	1.05	1.01	1.90	-0.08	0.03	0.69	0.97	1.18	1.68	-14.40
KANDI	TL	2.58	9.03	41.44	116.22	42.78	82.35	76.86	103.77	203.76	61.44	0.52	0.52
	Slope	0.46	0.78	1.21	0.99	1.63	0.81	1.52	0.96	1.08	1.51	-0.14	-0.00
NATITINGOU	TL	4.56	23.61	80.98	57.35	38.07	86.15	108.74	35.18	208.01	123.97	13.50	3.04
	Slope	0.96	0.67	0.86	2.06	1.55	0.31	2.38	1.75	0.98	1.10	5.77	-0.95
PARAKOU	TL	5.30	40.09	63.35	81.27	29.08	54.73	32.70	15.86	161.56	127.65	5.29	4.16
	Slope	0.52	0.98	1.37	0.58	1.76	0.62	2.73	-0.36	0.93	1.31	4.15	-3.16

Cotonou Station: Located further South and adjoining the Atlantic Ocean, this station experiences its first rains in March. The IPTA graph shows that rainfall increases from April to June (345 mm) and decreases from July to August (48 mm). It

rises again in September, peaking in October (approximately 160 mm), then declines until December-January, when rain is very rare. Two rainy seasons appear to be evident: one longer (April to June) and one shorter (September to October). These

results corroborate findings from [45-47], which identified two rainy seasons in Cotonou. It's important to note that the rainfall totals recorded in June and October are relatively higher in the second sub-period. Additionally, the amount of rain received in June at this station far exceeds that accumulated during other months, potentially causing flooding. Under these conditions, authorities are urged to take appropriate measures to protect people and their property during this month.

Regarding the rainfall difference between successive months, the figure shows that the arrows are almost all clustered in Regions I and III. The slopes are presented in Table 1. In Zone I, the transitions include J-F, F-M, M-A, A-M, M-J, A-S, and S-O, while in Zone III, the transitions are J-J, J-A, O-N, and N-D. It is evident that rainfall between September and October increases in both sub-periods, with a much stronger trend (slope = 11.01) in the second sub-period. These results indicate that it rains significantly more in October than in September during the second sub-period compared to the first sub-period, where the difference in rainfall is much smaller. Conversely, there is a decrease of about 50% in rainfall between March and April. While the rainfall difference between June and July is the most significant at this station, it is also noted that it is declining with a nearly equal trend in both sub-periods.

**Bohicon Station:** At this station, rainfall increases from March to July and then decreases in August, where it rains less compared to June and July. Rainfall rises again in September but then decreases once more until January, when it almost doesn't rain at all. Starting in February, rainfall resumes, but the totals remain low. According to the IPTA graph, the average monthly total decreases in April, while it experiences significant increases in March, June, July, September, and October. The TPSC shows that the transition from June to July has a relative decrease in the first sub-period, justifying its placement in the second zone. In Zone I, the transitions J-F, F-M, M-A, A-M, M-J, and A-S are found with varying slopes. The presence of these vectors in this region indicates an increase in rainfall between the aforementioned successive months in both sub-periods. The slopes exceed 1 (see Table 1) in F-M (1.30), A-M (4.80), M-J (1.36), and A-S (1.79), indicating a more significant rainfall transition between these successive months in the second sub-period. Conversely, a decrease in rainfall is noted between the months J-F (0.98) and M-A (0.35) within the same sub-period. The slopes obtained for M-A (0.35) and A-M (4.80) show that rainfall dropped by more than half between March and April and quintupled between April and May in the second sub-period. This phenomenon may be attributed to the delayed onset of the rainy season and can cause disruptions in agricultural scheduling, loss and/or decreased yields, and reduced income for producers.

Zone III encompasses the transitions from J-A, S-O, O-N, and N-D, indicating a downward trend in rainfall between these successive months found in this zone. The difference in

rainfall is much more significant between O-N and decreases almost similarly in both sub-periods. However, the rainfall difference between J-A (slope = 2.69) has nearly tripled during the second sub-period. This suggests that it rains less in August than in July during the second sub-period compared to the first sub-period, where the gap between the rainfall totals of July and August is much smaller.

**Save Station:** The rainy season starts in March and ends in October ([45]). The peak of monthly totals occurs in September. Rainfall totals in June, August, September, and October are relatively higher in the second sub-period, while only July shows a slight downward trend.

Regarding rainfall transitions between successive months, the vectors are distributed across all four zones. In Zone II, the vector D-J has a length of 7.22 mm with a slope of -14.64. Even though rainfall is very rare during this period, any precipitation that does occur is much more significant in December, particularly in the second sub-period. In Zone IV, the vector J-J shows a rainfall difference of 22.55 mm and a slope of -0.08, indicating almost no difference in rainfall between June and July in the second sub-period compared to the first.

Zone I includes half of the vectors, specifically J-F, F-M, M-A, A-M, M-J, and A-S. The rainfall difference is increasing with a nearly similar trend in both sub-periods, except for M-J, where the trend nearly doubled in the second sub-period. It rains twice as much in June as in May during the second sub-period.

Finally, in Zone III, the vectors J-A, S-O, O-N, and N-D are present. The highest rainfall difference is observed between October and November with a slope of 1.18, indicating a similar decrease in both sub-periods. The J-A vector shows a rainfall difference of about -60 mm between July and August in the first sub-period, while in the second sub-period, rainfall between the two months is similar.

In summary, rainfall evolves progressively from May to July, then slightly decreases in August before rising in September during the first sub-period. In the second sub-period, it gradually increases from May to June, stabilizes with significantly higher amounts until August, and then rises again in September.

**Natingou Station:** Located much further west, this station is influenced by the Atacora mountain range, which has an average elevation of 700 m. The first rains are recorded in March. Rainfall increases until August, where it peaks, and then gradually decreases until October. After this month, it rains almost not at all. In the rainy cycle, only April and July show a downward trend, while rainfall totals for May, June, August, September, and October are significantly on the rise. There is relatively less rain in April and July during the second sub-period. Conversely, much less rain falls in May, June, August, September, and October during the first sub-period.

Regarding the TPSC (Transitional Precipitation Cycle), the vectors indicating the transition between successive months are distributed in quadrants I and III, showing a nearly similar

trend during both sub-periods. In Zone I, the most significant transition is between July and August, with a slope of 2.38. The rainfall difference here is more than double in the second sub-period compared to the first.

Quadrant III shows a very high rainfall difference between September and October, which is the largest recorded difference at the station and is observed in both sub-periods. October clearly marks the end of the rainy season, with significantly lower rainfall compared to September totals.

Overall, it can be concluded that the rainy season starts in April and ends in October.

**Kandi Station:** Located further north in Benin, Kandi Station experiences a rainy season and a dry season. The first rains are recorded starting in April, but rainfall increases significantly from May, peaking in August before declining until October. According to the IPTA test, rainfall in June, August, September, and October shows a marked increase in the second sub-period, while May and July exhibit no trend. Significantly more rain falls in June, August, September, and October during this second sub-period.

Regarding the TPSC (Transitional Precipitation Cycle), the vectors indicating transitions between successive months are distributed in quadrants I and III, demonstrating a nearly similar trend during both sub-periods. Increasing transitions are observed in quadrant I, with the most significant transition between April and May having a slope close to 1, indicating similar evolution in both sub-periods.

In contrast, decreasing transitions appear in quadrant III, particularly between September and October, also with a slope of 1. It is clear that at Kandi Station, the transitions did not vary during the study period, even though some monthly totals exhibited trends.

**Parakou Station:** Located in the eastern part of the country, Parakou Station reflects the rainfall situation in northeastern Benin. The first rains are recorded starting in March, with significant accumulation beginning in April. Rainfall gradually increases until August, reaching its peak, then declines until October, marking the end of the rainy season. At this station, rainfall totals for April, September, and October are on the rise, while May and July show a downward trend. June and August do not exhibit significant trends. Regarding the TPSC (Transitional Precipitation Cycle), the vectors illustrating transitions between consecutive months are primarily distributed in quadrants I and III, showing similar transitions in both sub-periods. In quadrant I, the most significant transition is between April and May, with a slope of 0.58, indicating a decrease in rainfall between these two months during the second sub-period. Rainfall in recent decades has been less compared to the first sub-period. Although the gap between July and August is not large, there is a notable nearly threefold increase in the transition between these months, evidenced by a slope of 2.73. This transition has become much more significant in recent decades compared to the first sub-period. Quadrant III includes decreasing transitions, with the most important transition recorded between September and October, showing a

slope of about 1. Transitions identified in this quadrant decline at a similar rate in both sub-periods.

### 3.2. Discussion

This study focused on the trend of monthly rainfall at synoptic stations in Benin. The IPTA and TPSC methods were utilized to analyze hidden trends in rainfall across these stations. Significant seasonal patterns emerged, varying from one station to another, which may have important implications for agriculture and water resource management. The marked increase in rainfall during certain months, juxtaposed with decreases during others in the same rainy season, indicates a notable change in the country's traditional climate regime. This phenomenon cannot be ignored, especially given Benin's reliance on rain-fed agriculture. Rainfall is clearly bimodal in Cotonou, showing two rainy seasons [45, 46]. In contrast, other stations experience a single rainy season from March-April to October [45, 47]. This rainfall behavior could be interpreted through the movement of the Intertropical Front [45, 48].

The increase in precipitation during critical months of the rainy season may be viewed as an opportunity to enhance crop productivity. However, it could also have negative repercussions if it occurs during harvest time or when plants need less water [49-53].

On the other hand, the decrease in precipitation during July at the stations in Save, Natitingou, and Parakou - while the rainy season is ongoing- can induce water stress for certain crops that require a constant water supply [17]. Erratic fluctuations in rainfall patterns can adversely affect not only production [54-56] but also agricultural planning, necessitating adjustments in farming practices [51, 57]. For instance, farmers may need to adopt drought-resistant crop varieties or consider more sophisticated irrigation systems. Environmentally, the upward trend in rainfall may bring about flooding risks, particularly in June in Cotonou [58], in July in Bohicon and Save, and in August in areas around other stations. Flooding can lead to population migration [59, 60], exacerbated by conflicts [12] and economic losses. Socioeconomically, these rainfall variations impact the economy [3, 61, 62], potentially exacerbating existing inequalities among farmers. Smallholder farmers, who often lack the resources to adapt to climate changes, may suffer greater losses [62] compared to those with means to invest in resilient agricultural technologies. This could lead to increased food insecurity and social tensions in rural areas, where agriculture is the primary source of livelihood.

Furthermore, the health implications of rainfall variability must be considered [63-65], particularly due to the potential spread of waterborne diseases [66], such as cholera, which can thrive in conditions of heavy rain and flooding. Therefore, health infrastructures will need to be strengthened to adapt to these new climatic realities. To tackle the challenges posed by rainfall variability, an integrated approach is essential [67].

Collaboration among the government, NGOs, researchers, and local communities will be key in developing effective adaptation strategies. Policies that promote agricultural adaptation strategies based on favourable climatic conditions are encouraged to protect and enhance future agricultural production [68]. Agricultural policies should include water resource management measures, such as constructing drainage and retention systems to control excess water and maximize the use of water resources. Additionally, educating and raising awareness among farmers about sustainable and resilient farming techniques will be crucial for ensuring long-term food security. Building resilient cities to mitigate flooding and its consequences is also recommended.

## 4. Conclusions

The study of climate parameter variability through innovative methods is a key to better understanding the climate and making informed decisions. This research highlighted the variability of precipitation at synoptic stations in Benin using the IPTA method. It revealed hidden variability and rainfall transitions between successive months. The findings provide clear indicators for anticipating the impacts of rainfall variability, guiding mitigation and adaptation policies. They can also serve as a pragmatic guide for actions to take in response to an increasing global environmental challenge.

## Abbreviations

IPTA	Innovative Polygon Trend Analysis
MK	Mann-Kendall
TPSC	Trend Polygon Star Concept

## Author Contributions

**Hilaire Kougbegbede:** Conceptualization, Methodology, Validation, Writing – review & editing

**Mamadou Wa ïli Onah:** Methodology, Writing – original draft

**Arnaud Houeto:** Software, Visualization

**Ferdinand Sourou Hounvou:** Formal Analysis, Writing – review & editing

## Conflicts of Interest

The authors declare no conflicts of interest.

## References

- [1] Peters GP, Andrew RM, Boden T, Canadell JG, Ciais P, Le Quéré C, et al. The challenge to keep global warming below 2 °C. *Nat Clim Change* 2013; 3: 4–6. <https://doi.org/10.1038/nclimate1783>
- [2] Kundzewicz ZW. Extreme weather events and their consequences. *Pap Glob Change* 2016: 59–69.
- [3] Serdeczny O, Adams S, Baarsch F, Coumou D, Robinson A, Hare W, et al. Climate change impacts in Sub-Saharan Africa: from physical changes to their social repercussions. *Reg Environ Change* 2017; 17: 1585–600; <https://doi.org/10.1007/s10113-015-0910-2>
- [4] Bedair H, Alghariani MS, Omar E, Anibaba QA, Remon M, Bornman C, et al. Global Warming Status in the African Continent: Sources, Challenges, Policies, and Future Direction. *Int J Environ Res* 2023; 17: 45. <https://doi.org/10.1007/s41742-023-00534-w>
- [5] Zwane EM. Impact of climate change on primary agriculture, water sources and food security in Western Cape, South Africa. *J àmb áJ Disaster Risk Stud* 2019; 11. <https://doi.org/10.4102/jamba.v11i1.562>
- [6] Lobell DB, Burke MB, Tebaldi C, Mastrandrea MD, Falcon WP, Naylor RL. Prioritizing Climate Change Adaptation Needs for Food Security in 2030. *Science* 2008; 319: 607–10. <https://doi.org/10.1126/science.1152339>
- [7] Ebi KL, Ndebele-Murisa MR, Newsham AJ, Schleyer M. IPCC WGII AR5 Chapter 22. Africa 2014.
- [8] Maharjan A, De Campos RS, Singh C, Das S, Srinivas A, Bhuiyan MRA, et al. Migration and Household Adaptation in Climate-Sensitive Hotspots in South Asia. *Curr Clim Change Rep* 2020; 6: 1–16. <https://doi.org/10.1007/s40641-020-00153-z>
- [9] Piguet E, Pécoud A, De Guchteneire P. Migration and climate change: An overview. *Refug Surv Q* 2011; 30: 1–23.
- [10] Piguet E. Changements environnementaux et migration en Afrique de l'Ouest. Une revue des études de cas. *Belgeo* 2018; 1–26; <https://doi.org/10.4000/belgeo.28836>
- [11] Mastrorillo M, Licker R, Bohra-Mishra P, Fagiolo G, Estes LD, Oppenheimer M. The influence of climate variability on internal migration flows in South Africa. *Glob Environ Change* 2016; 39: 155–69; <https://doi.org/10.1016/j.gloenvcha.2016.04.014>
- [12] Amadi VT, Vundamina MN. Migration and climate change in Africa: A differentiated approach through legal frameworks on the free movement of people. *Law Democr Dev* 2023; 27: 31–54; <http://dx.doi.org/10.17159/2077-4907/2023/idd.v27.2>
- [13] Badou DF, Yegbemey RN, Hounkpè J. Sectorial Climate Change Impacts and Adaptation in Benin. In: Leal Filho W, Luetz J, Ayal D, editors. *Handb. Clim. Change Manag.*, Cham: Springer International Publishing; 2021, p. 1–21. [https://doi.org/10.1007/978-3-030-22759-3\\_336-1](https://doi.org/10.1007/978-3-030-22759-3_336-1)
- [14] Dossou JF, Li XX, Sadek M, Sidi Almouctar MA, Mostafa E. Hybrid model for ecological vulnerability assessment in Benin. *Sci Rep* 2021; 11: 2449; <https://doi.org/10.1038/s41598-021-81742-2>
- [15] Biao EI. Assessing the impacts of climate change on river discharge dynamics in Oueme River Basin (Benin, West Africa). *Hydrology* 2017; 4: 47; <https://doi.org/10.3390/hydrology4040047>

- [16] Batablinlè L, Bazyomo SD, Badou FD, Jean H, Hodabalo K, Zakari D, et al. Climate, water, hydropower, wind speed and wind energy potential resources assessments using weather time series data, downscaled regional circulation models: A case study for Mono River Basin in the Gulf of Guinea region. *Renew Energy* 2024; 224: 120099; <https://doi.org/10.1016/j.renene.2024.120099>
- [17] Agbossou EK, Toukon C, Akponikpè PBI, Afouda A. Climate variability and implications for maize production in Benin: A stochastic rainfall analysis. *Afr Crop Sci J* 2012; 20: 493–503.
- [18] Akponikpe PBI, Tovihoudji P, Lokonon B, Kpadonou E, Amegnaglo J, Segnon AC, et al. Etude de Vulnérabilité aux changements climatiques du Secteur Agriculture au Bénin. Rep Prod Proj “Projet D’Appui Sci Aux Process Plans Natx D’Adaptation Dans Pays Francoph Moins Avancés D’Afrique Subsaharienne” Clim Anal GGmbH Berl 2019.
- [19] Haldar S, Choudhury M, Choudhury S, Samanta P. Trend analysis of long-term meteorological data of a growing metropolitan city in the era of global climate change. *Total Environ Res Themes* 2023; 7: 100056; <https://doi.org/10.1016/j.totert.2023.100056>
- [20] Patel A, Prajapati K, Chadsaniya J, Mehta D, Waikhom S. Innovative Polygon Trend Analysis Method: A Case Study of the South Gujarat Region. *J Environ Inform Lett* 2024; 11: 38–46; <https://doi.org/10.3808/jeil.202400121>
- [21] Ebodé VB, Mahé G, Amoussou E. Impact de la variabilité climatique et de l’anthropisation sur les écoulements de la Bénoué (nord Cameroun). *Proc Int Assoc Hydrol Sci* 2021; 384: 261–7; <https://doi.org/10.5194/piahs-384-261-2021>
- [22] Pendergrass AG, Knutti R, Lehner F, Deser C, Sanderson BM. Precipitation variability increases in a warmer climate. *Sci Rep* 2017; 7: 17966; <https://doi.org/10.1038/s41598-017-17966-y>
- [23] Goni IB, Taylor RG, Favreau G, Shamsudduha M, Nazoumou Y, Ngounou Ngatcha B. Groundwater recharge from heavy rainfall in the southwestern Lake Chad Basin: evidence from isotopic observations. *Hydrol Sci J* 2021; 66: 1359–71. <https://doi.org/10.1080/02626667.2021.1937630>
- [24] Hamed KH, Rao AR. A modified Mann-Kendall trend test for autocorrelated data. *J Hydrol* 1998; 204: 182–96; [https://doi.org/10.1016/S0022-1694\(97\)00125-X](https://doi.org/10.1016/S0022-1694(97)00125-X)
- [25] Mann HB. Nonparametric tests against trend. *Econom J Econom Soc* 1945: 245–59.
- [26] Kendall MG. Rank correlation methods. 1948.
- [27] Huang S-H, Mahmud K, Chen C-J. Meaningful trend in climate time series: A discussion based on linear and smoothing techniques for drought analysis in Taiwan. *Atmosphere* 2022; 13: 444.
- [28] Hu Y. Water tower of the Yellow River in a changing climate: toward an integrated assessment 2014.
- [29] Blain GC. Teste de Mann-Kendall: a necessidade de considerar a interação entre correlação serial e tendência. *Acta Sci Agron* 2013; 35: 393–402.
- [30] Hu Z, Liu S, Zhong G, Lin H, Zhou Z. Modified Mann-Kendall trend test for hydrological time series under the scaling hypothesis and its application. *Hydrol Sci J* 2020; 65: 2419–38. <https://doi.org/10.1080/02626667.2020.1810253>
- [31] Wang F, Shao W, Yu H, Kan G, He X, Zhang D, et al. Re-evaluation of the power of the Mann-Kendall test for detecting monotonic trends in hydrometeorological time series. *Front Earth Sci* 2020; 8: 14; <https://doi.org/10.3389/feart.2020.00014>
- [32] Kartal V, Nones M, Topcu E, Ariman S. Comparison of different techniques in determining groundwater levels trends in Türkiye. *Hydrol Process* 2024; 38: e15244. <https://doi.org/10.1002/hyp.15244>
- [33] Şen Z. Innovative Trend Analysis Methodology. *J Hydrol Eng* 2012; 17: 1042–6. [https://doi.org/10.1061/\(ASCE\)HE.1943-5584.0000556](https://doi.org/10.1061/(ASCE)HE.1943-5584.0000556)
- [34] Zekâ. Trend Identification Simulation and Application. *J Hydrol Eng* 2014; 19: 635–42. [https://doi.org/10.1061/\(ASCE\)HE.1943-5584.0000811](https://doi.org/10.1061/(ASCE)HE.1943-5584.0000811)
- [35] Şen Z. Hydrological trend analysis with innovative and over-whitening procedures. *Hydrol Sci J* 2017; 62: 294–305. <https://doi.org/10.1080/02626667.2016.1222533>
- [36] Kougbéagbede H. Detection of annual rainfall trends using innovative trend analysis method in Benin. *Int J Glob Warm* 2024; 32: 54–64. <https://doi.org/10.1504/IJGW.2024.135361>
- [37] Şen Z, Şişman E, Dabanlı I. Innovative polygon trend analysis (IPTA) and applications. *J Hydrol* 2019; 575: 202–10; <https://doi.org/10.1016/j.jhydrol.2019.05.028>
- [38] Şen Z. Conceptual monthly trend polygon methodology and climate change assessments. *Hydrol Sci J* 2021; 66: 503–12. <https://doi.org/10.1080/02626667.2021.188109>
- [39] Hussain F, Ceribasi G, Ceyhunlu AI, Wu R-S, Cheema MJM, Noor RS, et al. Analysis of precipitation data using innovative trend pivot analysis method and trend polygon star concept: a case study of Soan River Basin, Potohar Pakistan. *J Appl Meteorol Climatol* 2022; 61: 1861–80; <https://doi.org/10.1175/JAMC-D-22-0081.1>
- [40] Koycegiz C, Buyukyildiz M. Applications of innovative polygon trend analysis (IPTA) and trend polygon star concept (TPSC) methods for the variability of precipitation in Konya Closed Basin (Turkey). *Theor Appl Climatol* 2024; 155: 2641–56. <https://doi.org/10.1007/s00704-023-04765-x>
- [41] Qadem Z, Tayfur G. In-depth Exploration of Temperature Trends in Morocco: Combining Traditional Methods of Mann Kendall with Innovative ITA and IPTA Approaches. *Pure Appl Geophys* 2024; 181: 2717–39. <https://doi.org/10.1007/s00024-024-03535-8>
- [42] Akcay F, Bingölbali B, Akpınar A, Kankal M. Trend detection by innovative polygon trend analysis for winds and waves. *Front Mar Sci* 2022; 9: 930911; <https://doi.org/10.3389/fmars.2022.930911>

- [43] Yenice AC, Yaqub M. Trend analysis of temperature data using innovative polygon trend analysis and modeling by gene expression programming. *Environ Monit Assess* 2022; 194: 543. <https://doi.org/10.1007/s10661-022-10156-y>
- [44] Ahmed N, Wang G, Booij MJ, Ceribasi G, Bhat MS, Ceyhunlu AI, et al. Changes in monthly streamflow in the Hindukush–Karakoram–Himalaya Region of Pakistan using innovative polygon trend analysis. *Stoch Environ Res Risk Assess* 2022; 36: 811–30. <https://doi.org/10.1007/s00477-021-02067-0>
- [45] Djossou J, Akpo A, Affévélé J, Donnou V, Lioussé C, Léon J-F, et al. Dynamics of the inter tropical front and rainy season onset in Benin. *Curr J Appl Sci Technol* 2017; 24: 1–15; <https://doi.org/10.9734/CJAST/2017/36832>
- [46] Boko M. Saisons et types de temps au Bénin: analyse objective et perceptions populaires. *Espace Géographique* 1992; 321–32.
- [47] Ahokossi Y. Analysis of the rainfall variability and change in the Republic of Benin (West Africa). *Hydrol Sci J* 2018; 63: 2097–123. <https://doi.org/10.1080/02626667.2018.1554286>
- [48] Rauch M, Bliedernicht J, Laux P, Salack S, Waongo M, Kunstmann H. Seasonal forecasting of the onset of the rainy season in West Africa. *Atmosphere* 2019; 10: 528; <https://doi.org/10.3390/atmos10090528>
- [49] Rembold F, Kerdiles H, Lemoine G, Perez-Hoyos A. Impact of El Niño on agriculture in Southern Africa for the 2015/2016 main season. *Jt Res Cent JRC MARS Bull Outlook Ser Eur Comm Bruss* 2016; <https://doi.org/10.1016/j.agry.2018.07.002>
- [50] Coleman A. High rainfall causes extensive damage to summer grain crop. *Farmers Wkly* 2022; 17.
- [51] Yegbemey RN, Yabi JA, Aihounton GB, Paraiso A. Simultaneous modelling of the perception of and adaptation to climate change: the case of the maize producers in northern Benin. 2014; <https://doi.org/10.1016/j.agry.2013.08.002>
- [52] Baffour-Ata F, Tabi JS, Sangber-Dery A, Etu-Mantey EE, Asamoah DK. Effect of rainfall and temperature variability on maize yield in the Asante Akim North District, Ghana. *Curr Res Environ Sustain* 2023; 5: 100222; <https://doi.org/10.1016/j.crsust.2023.100222>
- [53] Li Y, Guan K, Schnitkey GD, DeLucia E, Peng B. Excessive rainfall leads to maize yield loss of a comparable magnitude to extreme drought in the United States. *Glob Change Biol* 2019; 25: 2325–37. <https://doi.org/10.1111/gcb.14628>
- [54] Omoyo NN, Wakhungu J, Oteng'i S. Effects of climate variability on maize yield in the arid and semi arid lands of lower eastern Kenya. *Agric Food Secur* 2015; 4: 8. <https://doi.org/10.1186/s40066-015-0028-2>
- [55] Mapfumo P, Chagwiza C, Antwi M. Impact of rainfall variability on maize yield in the KwaZulu-Natal, North-West and Free State provinces of South Africa (1987–2017). *J Agribus Rural Dev* 2020; 58: 359–67.
- [56] Kinda SR, Badolo F. Does rainfall variability matter for food security in developing countries? *Cogent Econ Finance* 2019; 7: 1640098. <https://doi.org/10.1080/23322039.2019.1640098>
- [57] Chapman S, E Birch C, Pope E, Sallu S, Bradshaw C, Davie J, et al. Impact of climate change on crop suitability in sub-Saharan Africa in parameterized and convection-permitting regional climate models. *Environ Res Lett* 2020; 15: 094086; <https://doi.org/10.1088/1748-9326/ab9daf>
- [58] Badou DF, Hounkanrin J, Hounkpè J, Sintondji LO, Emmanuel Lawin A. Assessing the Return Periods and Hydroclimatic Parameters for Rainwater Drainage in the Coastal City of Cotonou in Benin under Climate Variability. *Adv Meteorol* 2023; 2023: 1–10. <https://doi.org/10.1155/2023/1752805>
- [59] Nourali Z, Shortridge JE, Bukvic A, Shao Y, Irish JL. Simulation of Flood-Induced Human Migration at the Municipal Scale: A Stochastic Agent-Based Model of Relocation Response to Coastal Flooding. *Water* 2024; 16: 263; <https://doi.org/10.3390/w16020263>
- [60] Almulhim AI, Alverio GN, Sharifi A, Shaw R, Huq S, Mahmud MJ, et al. Climate-induced migration in the Global South: an in depth analysis. *Npj Clim Action* 2024; 3: 47; <https://doi.org/10.1038/s44168-024-00133-1>
- [61] Ali S. Climate change and economic growth in a rain-fed economy: how much does rainfall variability cost Ethiopia? Available SSRN 2018233 2012; <http://dx.doi.org/10.2139/ssrn.2018233>
- [62] Sangkhaphan S, Shu Y. The effect of rainfall on economic growth in Thailand: a blessing for poor provinces. *Economies* 2019; 8: 1; <https://doi.org/10.3390/economies8010001>
- [63] Noji EK. Natural Disasters. *Crit Care Clin* 1991; 7: 271–92. [https://doi.org/10.1016/S0749-0704\(18\)30306-3](https://doi.org/10.1016/S0749-0704(18)30306-3)
- [64] Palmer PI, Wainwright CM, Dong B, Maidment RI, Wheeler KG, Gedney N, et al. Drivers and impacts of Eastern African rainfall variability. *Nat Rev Earth Environ* 2023; 4: 254–70; <https://doi.org/10.1038/s43017-023-00397-x>
- [65] Control C for D, Prevention (CDC. Morbidity and mortality associated with Hurricane Floyd–North Carolina, September–October 1999. *MMWR Morb Mortal Wkly Rep* 2000; 49: 369–72.
- [66] Dimitrova A, McElroy S, Levy M, Gershunov A, Benmarhnia T. Precipitation variability and risk of infectious disease in children under 5 years for 32 countries: a global analysis using Demographic and Health Survey data. *Lancet Planet Health* 2022; 6: e147–55; [https://doi.org/10.1016/S2542-5196\(21\)00325-9](https://doi.org/10.1016/S2542-5196(21)00325-9)
- [67] Egah J, Yegbemey RN, Idrissou FA, Baco MN. Eliciting indigenous knowledge to predict climate events for the food security of agro-pastoral households in North Benin. *Front Environ Econ* 2023; 2: 1134864; <https://doi.org/10.3389/fevc.2023.1134864>
- [68] Carr TW, Mkuhlani S, Segnon AC, Ali Z, Zougmore R, Dangour AD, et al. Climate change impacts and adaptation strategies for crops in West Africa: a systematic review. *Environ Res Lett* 2022; 17: 053001; <https://doi.org/10.1088/1748-9326/ac61c8>